Response to RC2

We sincerely thank the reviewers for their thorough and constructive evaluation of our manuscript. We have carefully considered all the comments and have substantially revised the manuscript accordingly. Below we provide point-by-point responses to all major and minor comments.

Response to Major Comments

1. C60 is used as a proxy for carbonaceous aerosols, but it is not representative of real particles (mainly amorphous carbon with functional groups). The authors should justify this choice and discuss potential overestimation of π-π interactions and underestimation of polar interactions. Including a complementary simulation with a more realistic model (e.g., amorphous carbon) would strengthen the work.

Response: We thank the reviewer for this critical and constructive comment. We fully agree that C60 is an idealized model and does not fully represent the complexity of real atmospheric carbonaceous particles, which are predominantly amorphous carbon with various surface functional groups, defects, and heteroatoms. We acknowledge that C60 may overestimate π-π interactions due to its highly symmetric, defect-free structure, while potentially underestimating polar interactions involving surface oxygen-containing functional groups, and that its smooth, closed-cage surface does not capture the microporous and morphological complexity of real soot or black carbon surfaces. However, C60 was selected specifically to isolate specific non-covalent interactions—namely π-π stacking, C–H···π hydrogen bonds, and dipole-π interactions—from the confounding effects of surface heterogeneity.

The use of fullerene as a surrogate for soot nanoparticles has precedent in the literature; for example, Ruan et al. (2023) employed C60 as a substitute for soot particles to investigate the growth of coronene radical, noting that fullerene is similar in structure to soot particles with a surface that can be treated as curved PAHs, and a study on new particle formation used fullerenes as model compounds to represent nanoparticles of soot (Liu et al. 2016). The uniform π-electron surface of C60 allows unambiguous identification of these interaction types at the molecular level—a task extremely difficult with real carbonaceous surfaces due to their chemical heterogeneity and morphological complexity.

We also acknowledge the reviewer's suggestion regarding complementary simulations; while we agree that simulations with more realistic carbon models would be valuable, such simulations present significant challenges due to the structural diversity of real amorphous carbon and the lack of well-validated force field parameters. Nevertheless, we have added this as a recommended future direction in the Conclusions. In the revised manuscript, we have added a discussion of the rationale and limitations of C60 in the Introduction, and expanded the limitations paragraph in the Conclusions to explicitly acknowledge potential overestimation/underestimation of interactions and the need for complementary simulations:

(1) 1 Introduction

"However, such understanding remains limited for nitrophenols on carbonaceous sur-faces. Real atmospheric carbonaceous particles, such as black carbon and

soot—which are products of incomplete combustion of fossil fuels or biomass—exhibit significant complexity in both chemical composition and physical structure. Their polyaromatic (graphite-like) surfaces can form π-π electron donor-acceptor complexes with nitroaromatic compounds, yet the adsorptive strength depends greatly on pyrolysis temperature, formation conditions, and subsequent environmental weathering. Moreover, the filling of micropores and mesopores is subject to steric effects due to size exclusion, and the adsorptive capacity becomes attenuated by fouling with natural organic matter that blocks pores and competes for adsorption sites. These factors, together with the chemical heterogeneity (oxygen-containing functional groups, defect sites, metal impurities) and morphological complexity (aggregates, pore structures) of real aerosol particles, make it extremely difficult to decouple adsorption from partitioning contributions or to identify specific non-covalent interaction types at the molecular level. Consequently, a well-defined model system is needed to isolate the specific interactions from the confounding effects of surface heterogeneity."

(2) 4 Conclusion

"The C60 aerosol surrogate, while useful for isolating specific non-covalent interactions, does not capture the full chemical complexity of real atmospheric particles—particularly the presence of oxygen-containing functional groups, surface defects, and heteroatoms that may enhance polar interactions. As a result, the C60 model may overestimate the contribution of π-π interactions and underestimate the role of polar interactions. Future complementary simulations using more realistic

carbon models, such as amorphous carbon clusters or graphene with functional groups, would be valuable to validate the trends identified here."

2. The authors note the concentration gap between O_2 and NO_2 but do not perform the necessary competition calculation. Given that O_2 (~0.2 atm, ~5×10^{18} cm^{-3}) is about $10^8 \sim 10^9$ times more abundant than NO_2 (~ppb, ~10^{10} cm^{-3}), the effective rate ($k \times$ [oxidant]) must be computed to identify the dominant pathway.

Response: We thank the reviewer for this critical comment. In the revised manuscript, we have added a quantitative analysis to Section 3.1.3: "It should be emphasized that the competition between O_2 and $\bullet NO_2$ for IM3' must be evaluated based on effective rates ($k \times$ [oxidant]) rather than second-order rate constants alone. The atmospheric concentration of O_2 is 5.4×10^{18} molecules cm^{-3} (0.21 atm). For the reaction of IM3' with O_2 via HAA (barrier = 2.86 kcal mol^{-1}), the barrier height indicates that the reaction is near the gas-kinetic limit, with rate constants for alkyl radical + O_2 reactions typically in the range of $10^{-12} \sim 10^{-11}$ cm^3 $molecule^{-1}$ s^{-1} (Miyoshi et al., 1990; Morgan et al., 1982). Taking a conservative estimate of $kO_2 \approx 10^{-12}$ cm^3 $molecule^{-1}$ s^{-1}, the effective rate is $k'O_2 \approx 10^{-12} \times 5.4 \times 10^{18} \approx 5.4 \times 10^6$ s^{-1}, corresponding to a lifetime of 0.2 microseconds—consistent with the well-established behavior that alkyl radicals react with O_2 on timescales of 10 ~ 100 nanoseconds (Vereecken and Francisco, 2012; Calvert et al., 2015). For the reaction of IM3' with $\bullet NO_2$ via HAA (barrier = 2.01 kcal mol^{-1}), even under the most favorable nighttime conditions with [$\bullet NO_2$] ≈ $10^{10} \sim 10^{11}$ molecules cm^{-3}, and taking $kNO_2 \approx 10^{-11}$ cm^3 $molecule^{-1}$ s^{-1}, the effective rate is $k'NO_2 \approx 10^{-1} \sim 1$ s^{-1}, corresponding to a lifetime of

1 ~ 10 seconds. Thus, $k'O_2$ is more than 6 orders of magnitude faster than $k'NO_2$. The overwhelming concentration advantage of O_2—more than 10^7 times that of $\bullet NO_2$—ensures that the reaction of IM3' with O_2 is the dominant atmospheric fate of this intermediate. This is fully consistent with the established behavior that addition of O_2 is essentially the sole atmospheric fate of organic radicals formed during the oxidation of organic compounds (Calvert et al., 2015)."

3. The 1 ns MD production run is too short for this complex interface. I recommend extending the simulation to at least 10–20 ns and showing convergence plots (e.g., RMSD and total energy vs. time). The choice of the AMBER99SB-ILDN + GAFF force field also needs justification, especially for polarisation in aromatic–fullerene interactions; benchmarking against a polarisable force field or ab initio MD would increase confidence.

Response: We thank the reviewer for this critical comment. We fully acknowledge that longer simulations and polarizable force fields would be desirable. However, we respectfully argue that the current 1 ns simulation with AMBER99SB-ILDN + GAFF is scientifically justified for this specific system, for the following reasons.

First, regarding simulation length. The adsorption energy converged within 500 ps and remained stable throughout the 1 ns trajectory (Figure 6c). The key non-monotonic trend was consistently reproduced across four independent replicas at each hydration level, confirming statistical robustness. For small rigid molecules on rigid surfaces such as C60, the conformational space is limited and equilibrium is

typically reached on the sub-ns timescale. In addition, we have extended the simulations to 5 ns and confirmed that the adsorption energy trend remains unchanged, indicating that 1 ns is sufficient for the properties of interest. The consistency across replicas, rather than the absolute simulation length, provides the statistical confidence for our conclusions.

Second, regarding force field choice. AMBER99SB-ILDN (Lindorff-Larsen et al. 2010) and GAFF (Wang et al. 2004) are among the most extensively validated force fields for organic systems. GAFF has been successfully applied to fullerene systems (Huy and Li, 2014) and nitroaromatic compounds. For C60-2,4-DNP interactions, the dominant contribution is van der Waals dispersion, which is well described by GAFF's Lennard-Jones parameters; electrostatic contributions are minor due to C60's neutral, symmetric nature. We acknowledge the limitation of non-polarizable force fields and have added a statement to this effect in the Conclusions, recommending future validation with polarizable force fields.

4. Before concluding that ozonolysis amplifies toxicity, the authors should first establish whether it is indeed the dominant atmospheric transformation pathway for 2,4-DNP. Moreover, the toxicity assessment relies solely on the T.E.S.T. QSAR tool; cross-validation with at least one independent model (e.g., ECOSAR, ADMETlab) is recommended, along with a clear discussion of applicability domains and prediction uncertainties. High-risk products such as IM54 should be explicitly prioritised for experimental validation.

Response: We thank the reviewer for this critical and constructive comment. We address each point in turn.

Regarding the dominance of ozonolysis as an atmospheric transformation pathway, we acknowledge that our kinetic calculations show the •OH pathway (gas-phase $k = 3.18 \times 10^{-15}$ cm^3 $molecule^{-1}$ s^{-1}) is the dominant daytime oxidant, while O_3 (gas-phase $k = 4.23 \times 10^{-23}$ cm^3 $molecule^{-1}$ s^{-1}) plays a less significant role under typical daytime conditions. However, we selected the ozonolysis pathway for toxicity assessment for two reasons: (i) O_3 reacts with aromatic rings via a relatively well-defined mechanism, producing a comparatively clear product spectrum, which allows for systematic identification of transformation products and their toxicity; and (ii) the •OH pathway generates a substantially more complex and diverse product mixture due to the multiple possible addition and abstraction sites, making a comprehensive toxicity comparison far more challenging. We have clarified this rationale in Section 3.3 of the revised manuscript.

Regarding cross-validation of QSAR predictions, we have performed an independent cross-validation using Toxtree (version 3.1.0), which employs rule-based structural alerts (Benigni/Bossa rules) that are algorithmically distinct from T.E.S.T.'s statistical consensus method. The cross-validation results (now summarized in Table S4 of the Supplement) show consistent predictions for the majority of compounds:

"Table S4. Cross-validation of Ames mutagenicity and developmental toxicity predictions for 2,4-DNP and its ozonolysis products using two independent QSAR

tools (T.E.S.T. and Toxtree). “ND” = not detected (negative), “D” = detected (positive), “NA” = not applicable / outside applicability domain.”

Compound	T.E.S.T	Toxtree
	Ames mutagenicity	
2,4-DNP	ND (0.13)	ND
IM17	NA (0)	ND
IM25	NA (0)	ND
IM44	NA (0)	ND
IM54	NA (0)	ND
P1	D (0.53)	ND
P2	ND (0.21)	D
P3	ND (0.47)	ND
P4	ND (0.21)	ND
	Developmental toxicity	
2,4-DNP	D (0.55)	D
IM17	D (0.67)	D
IM25	D (0.85)	D
IM44	D (0.84)	D
IM54	D (0.94)	D
P1	D (0.58)	D
P2	D (0.56)	D
P3	D (0.65)	D
P4	D (0.56)	D

Regarding the scope of application and the uncertainty of predictions and experimental validation of high-risk products, we have already discussed these issues in Section 3.3, providing detailed explanations specifically for these matters: The QSAR models utilized in this study provide valuable preliminary information for risk

prioritization, the inherent uncertainties associated with in silico predictions must be acknowledged. The predictive performance is fundamentally constrained by the chemical space of the training sets and the defined applicability domains. For structurally distinct species such as 2,4-DNP and its various derivatives, the confidence levels of the predictions may be diminished because these models cannot fully elucidate specific toxicological modes of action. In addition, categorical predictions with probability scores close to threshold are inherently unstable, suggesting that the "not detected" Ames mutagenicity signals for intermediates such as IM17, IM25, IM44, and IM54 may reflect model limitations rather than a definitive absence of toxicity. These compounds should therefore be regarded as high-priority targets for experimental validation. Furthermore, these computational frameworks necessarily simplify complex biological endpoints such as developmental toxicity. Therefore, the present findings should be interpreted as hypothesis-generating rather than definitive. Future studies are recommended to validate these predictions through in vitro Ames tests and zebrafish embryo development experiments, and to develop targeted removal strategies for toxic nitrocarbonyl-type products.

5. The introduction cites many references but does not clearly define the central knowledge gap. The conclusion mostly restates the findings without offering concrete recommendations for modelling, monitoring, or experimental validation. Please sharpen the research question in the Introduction and add specific action-oriented suggestions in the Conclusion.

Response: We thank the reviewer for this comment. In the revised manuscript, we have sharpened the research question in the Introduction and added specific action-oriented recommendations in the Conclusions.

In the Introduction, we have revised the final paragraph to clearly articulate the central knowledge gap and the specific research questions: “Despite extensive studies on individual aspects of nitrophenol atmospheric chemistry, a systematic, molecular-level understanding of the multiphase fate of 2,4-DNP remains lacking. In particular, three key questions remain unanswered: (i) How do the two nitro substituents quantitatively alter the kinetics and selectivity of O_3, •OH, and •NO_2 reactions relative to mononitrophenols? (ii) How does interfacial hydration regulate the adsorption of 2,4-DNP on carbonaceous surfaces at the molecular level? (iii) Does oxidative processing of 2,4-DNP detoxify or potentially amplify the toxicity of the reaction products? To address these questions, this study employs an integrated multiscale theoretical framework combining density functional theory (DFT), molecular dynamics (MD) simulations, and computational toxicology to investigate the competing oxidation and nitration pathways of 2,4-DNP in gas and aqueous phases, its interfacial adsorption behavior on carbonaceous aerosol surrogates under different hydration conditions, and the toxicity evolution of its transformation products. The present work focuses exclusively on 2,4-DNP as a representative dinitrophenol, with the quantitative conclusions applying specifically to this compound, while the qualitative framework may provide a reference for understanding related nitroaromatic systems.”

In the Conclusions, we have added the following specific, action-oriented recommendations: “Based on these findings, we recommend the following directions for future research: (i) Experimental validation of predicted kinetics: Advanced kinetic techniques such as laser-induced fluorescence or cavity ring-down spectroscopy should be employed to measure the rate constants for the reactions of 2,4-DNP with O_3 and •OH, providing direct experimental confirmation of the theoretical trends. (ii) In vitro toxicity testing: The high-priority ozonolysis products identified in this study (IM54, P1, and P2) should be subjected to Ames mutagenicity assays and zebrafish embryo developmental toxicity tests to validate the QSAR predictions. (iii) Refined interfacial models: Complementary MD simulations using more realistic carbonaceous models, such as functionalized graphene or amorphous carbon clusters, would help assess the influence of surface functional groups and defects on the adsorption behavior of 2,4-DNP. (iv) Diurnal box model simulations: Full diurnal chemical box models incorporating temporally resolved oxidant concentrations, Henry’s law partitioning, and aerosol liquid water content are needed to fully quantify the atmospheric importance of each oxidation pathway under different pollution regimes. Despite these caveats, the mechanistic insights into the molecular-level reactivity and interfacial behavior of 2,4-DNP provide a foundation for future experimental and modeling studies on the multiphase fate of nitrophenolic compounds.”

Response to Minor Comments

1. Have the authors clearly described the methodology used to compute the

aqueous-phase rate constants?

Response: We thank the reviewer for this question. In the original manuscript, the methodology for computing rate constants is described in Section 2.3 (Kinetic calculations), where we explicitly state that the rate constants were calculated using the thermodynamic formulation of conventional transition state theory (TST), with support from the KiSThelP tool and the TST calculator, as represented by Eq. (1). The TST calculator referenced is a well-established tool developed by Tian Lu for calculating thermodynamic properties and rate constants from quantum chemistry results. This tool is capable of handling both gas-phase and solution-phase rate constant calculations, including aqueous-phase reactions under the 1 M standard state convention.

2. The statement "Green regions ($\Delta f\omega > 0$) … showing electrophilic features" is ambiguous. These regions indicate electron-poor sites that are susceptible to nucleophilic attack; please revise to avoid confusion.

Response: We thank the reviewer for this important clarification. We agree that the original statement "Green regions ($\Delta f\omega > 0$) showing electrophilic features" was ambiguous and could cause confusion. These regions indicate electron-poor sites with low electron density, which are susceptible to nucleophilic attack rather than being electrophilic species themselves.

In the revised manuscript, we have corrected the wording throughout Section 3.1.1 to accurately reflect the chemical meaning of the OWDD analysis. The specific revisions are as follows: "In contrast, green regions ($\Delta f\omega > 0$) are mainly located at

the outer ends of the oxygen and nitrogen atoms in the nitro and hydroxyl groups, indicating electron poor sites (low electron density) that are susceptible to nucleophilic attack, which arise from σ-hole interactions caused by the polarization of N–O and O–H bonds."

3. Figures 3 and 5: Energy units and axis labels are not clearly legible.

Response: We thank the reviewer for this comment. We have carefully revised Figures 3 and 5 to improve their clarity and legibility. The revised figures have been included in the updated manuscript.

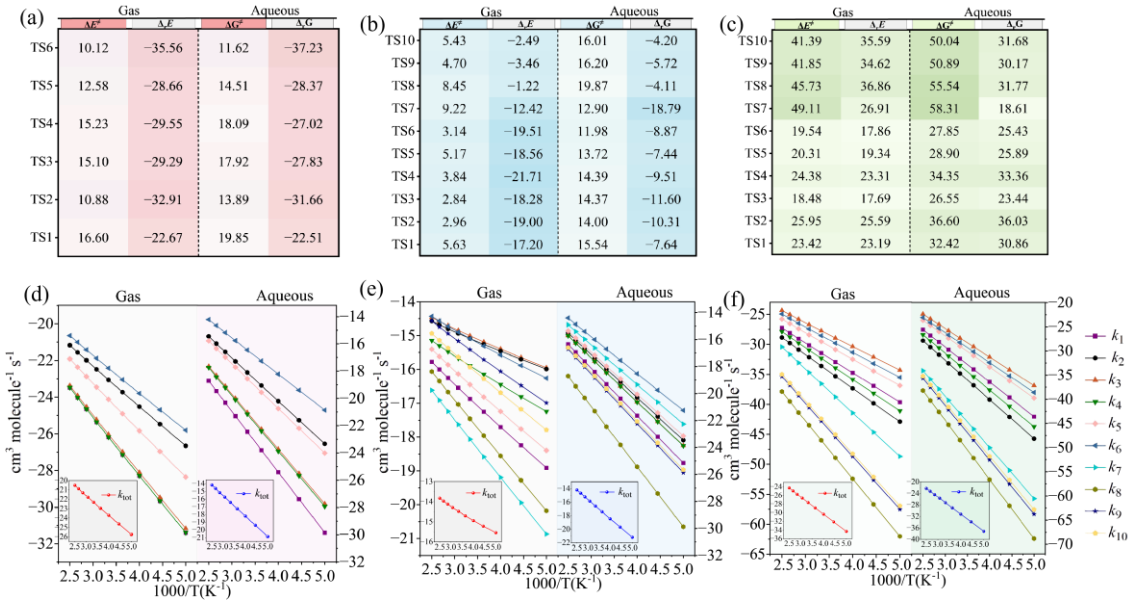

Figure 3 Thermodynamics, kinetics, and temperature dependence of the reactions of 2,4-DNP with O_3, •OH, and •NO_2. (a–c) reaction energy barriers ($\Delta E^{\neq}$) and reaction energies ($\Delta_r E$) for the key pathways (unit: kcal mol^{-1}). (d–e) Intrinsic temperature-dependent reaction rate constants for the major channels.

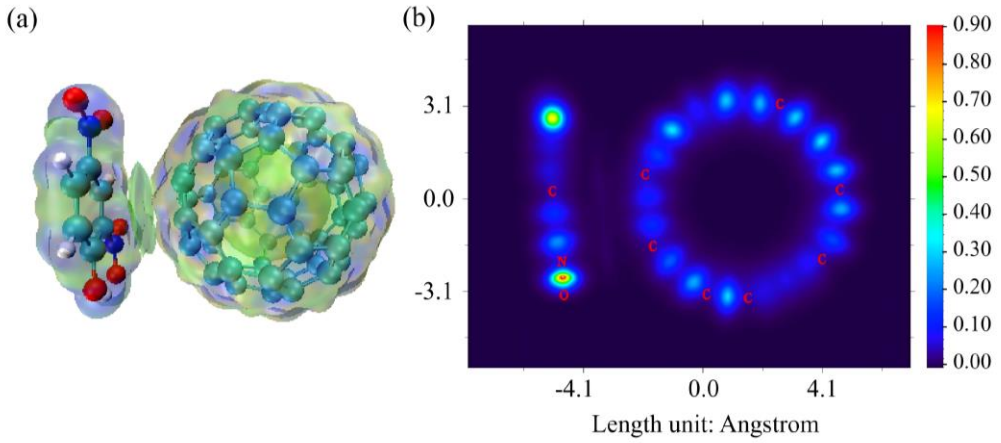

Figure 5 IGM analysis of intermolecular interactions in the 2,4-DNP-C60 aggregate. (a) three-dimensional (3D) IGM isosurface map. (b) Two-dimensional (2D) IGM density map.

4. Although Tables S1–S4 are mentioned, no concise visual summary or comparative plot is included in the main text to help readers quickly grasp the key data. It would be helpful to present a summary (e.g., a bar chart of rate constants or a table of key energy barriers) in the main paper, with full details left to the Supplement.

Response: We thank the reviewer for this constructive suggestion. To address this, we have added a new Table 2 in Section 3.1.2, which summarizes the calculated energy barriers, reaction energies for the most favorable reaction channels, and total rate constants at 298.15 K of 2,4-DNP with O_3, •OH, and •NO_2 in both gas and aqueous phases. This table highlights the dominant pathways and allows direct comparison of the relative reactivities of the three oxidants. Detailed data for all individual channels, including transition state geometries and vibrational frequencies,

remain available in Tables S1–S4 of the Supplement, as originally provided. The revised manuscript content is as follows:

"**Table 2** Summary of calculated energy barriers ($\Delta E^{\neq}$, kcal mol^{-1}), reaction energies ($\Delta_r E$, kcal mol^{-1}), and rate constants ($k$tot, cm^3 molecule^{-1} s^{-1}) at 298.15 K for the major reaction channels of 2,4-DNP with O_3, •OH, and •NO_2 in the gas and aqueous phases. Values in parentheses are for the aqueous phase. Detailed data for all channels are provided in Tables S1–S4 of the Supplement."

Oxidant	Channel	Phase	$\Delta E^{\neq}$	$\Delta_r E$	$k$tot (298 K)
O_3	R6 (C5=C6 addition)	Gas	10.12	–35.56	4.23×10^{-23}
		Aq.	11.62	–37.23	3.17×10^{-17}
•OH	R3' (addition at C3)	Gas	2.84	–18.28	3.18×10^{-15}
	R6' (addition at C6)	Aq.	11.98	–8.87	2.25×10^{-17}
•OH	R9' (HAA at C5)	Gas	4.70	–3.46	
	R9' (HAA at OH)	Aq.	12.90	–18.79	
•NO_2	R3* (addition at C3)	Gas	18.48	17.69	1.75×10^{-28}
		Aq.	26.55	23.34	3.93×10^{-28}
•NO_2	R10* (HAA at C6)	Gas	41.39	35.59	
		Aq.	50.04	31.68	

5. In summary, while this manuscript is rich in content, its overall logic is not clearly presented. The authors should explicitly state the specific research questions and scope of this study in the final paragraph of the Introduction.

Response: We thank the reviewer for this constructive suggestion. In the revised manuscript, we have substantially rewritten the final paragraph of the Introduction: "Despite extensive studies on individual aspects of nitrophenol atmospheric chemistry, a systematic, molecular-level understanding of the multiphase fate of 2,4-DNP remains lacking. In particular, three key questions remain unanswered: (i) How do the two nitro substituents quantitatively alter the kinetics and selectivity of O_3, •OH, and •NO_2 reactions relative to mononitrophenols? (ii) How does interfacial hydration regulate the adsorption of 2,4-DNP on carbonaceous surfaces at the molecular level? (iii) Does oxidative processing of 2,4-DNP detoxify or potentially amplify the toxicity of the reaction products? To address these questions, this study employs an integrated multiscale theoretical framework combining density functional theory (DFT), molecular dynamics (MD) simulations, and computational toxicology to investigate the competing oxidation and nitration pathways of 2,4-DNP in gas and aqueous phases, its interfacial adsorption behavior on carbonaceous aerosol surrogates under different hydration conditions, and the toxicity evolution of its transformation products. The present work focuses exclusively on 2,4-DNP as a representative dinitrophenol, with the quantitative conclusions applying specifically to this compound, while the qualitative framework may provide a reference for understanding related nitroaromatic systems.

Calvert, J. G., Orlando, J. J., Stockwell, W. R., and Wallington, T. J.: *The Mechanisms of Reactions Influencing Atmospheric Ozone*, Oxford University Press, New York, 2015.

Lindorff-Larsen, K., Piana, S., Palmo, K., Maragakis, P., Klepeis, J. L., Dror, R. O., and Shaw, D. E.: Improved side-chain torsion potentials for the Amber ff99SB protein force field, *Proteins*, 78, 1950–1958, 2010.

Liu, Y., Wang, Z., Wang, S., Fang, H., and Wang, D.: Soot nanoparticles could partake in nucleation of biogenic particles in the atmosphere: using fullerene as a model compound, *Atmosphere*, 7, 45, 2016.

Miyoshi, A., Matsui, H., and Washida, N.: Rates of reaction of hydroxyalkyl radicals with molecular oxygen, *J. Phys. Chem.*, 94, 3016–3019, 1990.

Morgan, C. A., Pilling, M. J., Tulloch, J. M., Ruiz, R. P., and Bayes, K. D.: Direct measurements of the rates of reaction of alkyl radicals with O_2, *J. Chem. Soc., Faraday Trans. 2*, 78, 1323–1332, 1982.

Ruan, S. S., Shi, Y., Qin, C. L., Xu, K. W., He, C. L., and Zhang, L. D.: A theoretical study on the effect of C60 particles on the growth of coronene radical based on HACA pathway, *Phys. Chem. Chem. Phys.*, 25, 16550–16558, 2023.

Vereecken, L. and Francisco, J. S.: Theoretical studies of atmospheric reaction mechanisms in the troposphere, *Chem. Soc. Rev.*, 41, 6259–6293, 2012.

Wang, J., Wolf, R. M., Caldwell, J. W., Kollman, P. A., and Case, D. A.: Development and testing of a general amber force field, *J. Comput. Chem.*, 25, 1157–1174, 2004.